PELLET AND GAS-PUFF FUELING SIMULATION IN ITER AND POWER PLANT PLASMAS USING "TOTAL" CODE

Tetsutarou Oishi, Kozo Yamazaki, Hiroaki Yamamoto, Hideki Arimoto and Tatsuo Shoji

Nagoya University, Chikusa-ku, Nagoya 464-8603 Japan

The efficiency of pellet injection and the relationship between D/T fuel ratio and plasma parameters were analyzed numerically using the TOTAL (toroidal transport analysis linkage) simulation code, which consists of the equilibrium calculation code and a one-dimensional transport simulation model. The simulation which included scanning the pellet penetration depth and the pellet D/T ratio was performed for a D-T fusion reactor designed like ITER. Deep penetration of the pellet was confirmed to be effective for suppressing anomalous transport and for forming the internal transport barrier. The operational region of temperature and density varies with the D/T ratio in the pellet.

1. Introduction

The deuterium/tritium fuel ratio is a key parameter to determine fusion energy reactor- characteristics such as plasma density and temperature or the output power. To control the D/T fuel ratio, several methods using the fuel supply of a nuclear fusion reactor, such as pellet injection, neutral beam injection, or gas puffing, have been proposed.

To analyze the efficiency of pellet injection and the relationship between the D/T fuel ratio and plasma parameters numerically, we apply the TOTAL (toroidal transport analysis linkage) [1] simulation code for the modeling of fuel supply in the D-T burning plasmas. The 2-dimensional or 3-dimensional equilibrium calculation using APOLLO [2] or VMEC [3] code, and the one-dimensional transport simulation model, are combined in the TOTAL code.

2. Simulation Methods

2.1. Transport Model

We have employed a transport model considering the suppression of turbulence by $E \times B$ shear and the resulting improvement of confinement [4]. This model focuses on the ion temperature gradient (ITG) mode [5] as the representative turbulence. The thermal diffusion coefficient χ is determined as

$$\chi = \chi_{NC} + \chi_{AN} \times F(\omega_{E \times B} / \gamma_{ITG}),\qquad(1)$$

where χ_{NC} and χ_{AN} are the neoclassical and anomalous thermal diffusion coefficients, respectively. Neoclassical components were calculated using the formula including the effect of the finite aspect ratio suggested by C. S. Chan

and F. L. Hinton [6]. In the present study, the Bohm and Gyro-Bohm mixed model [7] is employed to express χ_{AN},

$$\chi_{AN} = 4.0 \chi_{Bohm} + 0.5 \chi_{Gyro-Bohm},\qquad(2)$$

$$\chi_{Bohm} = 4 \times 10^{-5} R \left| \frac{\nabla(n_e T_e)}{n_e B_\phi} \right| q^2,\qquad(3)$$

$$\chi_{Gyro-Bohm} = 5 \times 10^{-6} \sqrt{T_e} \left| \frac{\nabla T_e}{B_\phi^2} \right|.\qquad(4)$$

Each proportional coefficient for χ_{Bohm} and $\chi_{Gyro-Bohm}$ was determined by a comparison with the experimental data of the reversed shear discharge of JT-60U tokamak [8]. Discharges including ITB formation were used as reference data (#29728, #32423). The factor $[(T_e \ (\rho = 0.8) - T_e \ (\rho = 1.0)) / T_e \ (\rho = 1.0)]$ is multiplied to χ_{Bohm} to express the edge effect of H-mode behavior in this calculation.

$F(\omega_{ExB}/\gamma_{ITG})$ in Eq. (1) is the improvement factor [9] defined as

$$F(\omega_{E \times B} / \gamma_{ITG}) = \frac{1}{1 + (\omega_{E \times B} / \gamma_{ITG})^2}.\qquad(5)$$

ω_{ExB} is the $E \times B$ flow shearing rate [10] defined as

$$\omega_{E \times B} = \left| \frac{RB_\theta}{B_\phi} \frac{\partial}{\partial r} \left(\frac{E_r}{RB_\theta} \right) \right|,\qquad(6)$$

and γ_{ITG} is the linear growth rate of the ITG mode defined as

$$\gamma_{ITG} = \frac{(\eta_i - 2/3)^{1/2} |s| c_i}{qR}, \tag{7}$$

where $\eta_i = L_n / L_T$ is the ratio between ion density scale length L_n and ion temperature scale length L_T, s is the magnetic shear defined by

$$s = \frac{r}{q} \left(\frac{dq}{dr} \right), \tag{8}$$

and $c_i = (T_i/m_i)^{1/2}$ [5]. From Eqs. (1) and (5), we can understand that the anomalous transport is suppressed when ω_{ExB} exceeds γ_{ITG}.

The anomalous part of the particle diffusion coefficient D_{AN} is calculated as

$$D_{AN} = (0.3 + 0.7\rho) \frac{\chi_{eAN} \chi_{iAN}}{\chi_{eAN} + \chi_{iAN}}. \tag{9}$$

For the impurity transport, neoclassical components were calculated using the NCLASS code [11] and anomalous components were given as input values. Carbon and tungsten are included as the species of impurity.

2.2. Pellet Injection Model

It is widely recognized that the pellet injection from the high-field-side (HFS) is effective for injecting pellets deep into the core region of tokamak plasma [12]. To simulate HFS pellet injection, we apply the "neutral gas shielding (NGS) model" [13], which describes pellet ablation, and the "mass relocation model" [14], which describes the drift of plasmoid generated by pellet ablation.

The NGS model gives the ablation rate along the pellet path l as

$$\frac{dN}{dl} = 4.38 \times 10^3 N^{0.444} n_e^{0.333} T_e^{1.64} M_i^{-0.333} / V_p, \tag{10}$$

where N is the number of atoms in a pellet, M_i is the pellet mass, and V_p is the pellet injection velocity.

The mass relocation model gives the displacement δx ($x = r/a$, normalized minor radius) of plasmoid in the major-radius direction as

$$\delta x = \delta r / a \sim \delta \psi / \Delta \psi, \tag{11}$$

where ψ, $\delta \psi$, and $\Delta \psi$ are the poloidal flux, the poloidal flux perturbation, and the total poloidal flux, respectively. $\delta \psi$ is obtained by the scaling

$$\delta \psi = q \beta B_\phi (1 + qL_c / a)^{-1} a^{-1} \delta n r_0^2 (n + \langle \delta n \rangle)^{-1}, \tag{12}$$

and $\Delta \psi$ is

$$\Delta \psi = \psi(a) - \psi(0) \sim \int r dr / q, \tag{13}$$

where r_0 and L_c are the radius and height of the cylindrical plasmoid, respectively.

3. Simulation Results

The plasma parameters of an ITER-like tokamak reactor with reversed shear configuration as simulation targets are determined using the reactor design system PEC (Physics-Engineering-Cost) code [15]. The main plasma parameters are shown in Table 1. These parameters refer to the 1GW electric power generated by the D-T reaction. In this simulation, pellet injection frequency and auxiliary heating power are feedback-controlled such that the density and temperature increase in the initial state, and then the alpha particle heating power keeps a value of 600 MW during the steady state.

Table 1. Plasma parameters of the tokamak reactor used in the present study.

major radius R_p [m]	5.29
minor radius a_p [m]	1.25
toroidal field B_{z0} [T]	7.11
plasma current I_p [MA]	13.0
α heating power [MW]	600.0
ellipticity	2.0
triangularity	0.5

At first in this section, we investigated the condition of pellet injection to form ITB. We then examine the behavior of parameters in the burning plasma accompanying the variation in the D/T ratio in the pellet.

3.1. Effect of pellet injection depth

Figure 1 shows the simulation results of the reversed shear tokamak reactor with pellet-injection fuelling. The pellet is penetrated up to $\rho = 0.4$ (a "deep penetration case"). It corresponds to the normalized penetration length $\lambda_{pel} = 0.6$. The left-hand side of Fig. 1 shows the temporal evolutions of (a) the alpha heating power P_α, auxiliary heating power P_{heat}, the radiation power loss P_{rad}, (b) averaged electron density $\langle n_e \rangle$, electron temperature $\langle T_e \rangle$, and ion temperature $\langle T_i \rangle$. At the steady state after 60 sec, $\langle n_e \rangle \sim 2 \times 10^{20}$ m^{-3} and $\langle T_e \rangle \sim \langle T_i \rangle \sim 20$ keV. Figure 1(c) shows the radial profile of electron density n_e, electron temperature T_e, ion temperature T_i, and pellet deposition Δn_e. One can see that both the density and the temperature profile have a steep gradient at $\rho = 0.55 \sim 0.7$. The pellet ablation

profile shows that the pellet penetrated up to $\rho = 0.4$. Now we include the value λ_{pel} as an indicator of the penetration depth measured from the plasma edge, which is normalized by the plasma minor radius. Namely, $\lambda_{pel} = 1$ indicates that the pellet has reached the plasma center. The case shown in Fig. 1 corresponds to $\lambda_{pel} = 0.6$. Figure 1(d) shows the growth rate of the ion temperature gradient mode γ_{ITG} and the E x B shearing rate ω_{ExB}. ω_{ExB} exceeds γ_{ITG} at $\rho = 0.55{\sim}0.7$, which corresponds to the region of ITB formation.

On the other hand, ITB is not formed if the pellet penetration depth is shallow. Figure 2 shows the result of simulation in a case where the pellet is penetrated up to $\rho = 0.7$, corresponding to $\lambda_{pel} = 0.3$. As shown in Fig. 2(d), γ_{ITG} is larger than ω_{ExB} at almost all regions. The suppression of turbulence does not occur and confinement is not improved. The temperature increase is not sufficient, as shown in Fig. 2(b), $\langle T_e \rangle \sim \langle T_i \rangle \sim 10$ keV. Therefore, high density is required to achieve ignition. However, $\langle n_e \rangle$ in the steady burning state of about 4×10^{20} m^{-3} exceeds the Greenwald density limit of 2.65×10^{20} m^{-3} calculated using $I_p = 13$ MA and $a_p = 1.25$ m. Therefore, one can see that this operation

scenario is not feasible.

To investigate the relationship between the pellet penetration depth λ_{pel} and the formation of ITB, simulation with scanning λ_{pel} was conducted. The open circles in Fig. 3 show the maximum values of normalized electron temperature gradient R/L_{Te} for various λ_{pel}. Larger R/L_{Te} corresponds to clearer ITB formation. As the figure shows, ITB is formed in the cases that $\lambda_{pel} > 0.35$. The filled circles in Fig. 3 show the normalized minor radius ρ where R/L_{Te} becomes the maximum value. In cases where ITB is formed, the normalized minor radius having the maximum R/L_{Te} is around 0.65 and does not vary significantly. At $\rho = 0.65$, the magnetic shear is almost zero and γ_{ITG} is small. Therefore, if there is large

Fig.2 Simulation results of the reversed shear tokamak reactor with fuelling by pellet injection. The pellet is penetrated up to $\rho = 0.7$ ("shallow penetration case"). This corresponds to $\lambda_{pel} = 0.3$. The left figures show the temporal evolutions of (a) P_α, P_{heat}, P_{rad}, (b) $\langle n_e \rangle$, $\langle T_e \rangle$, and $\langle T_i \rangle$. The right figures show the radial profiles of (c) n_e, T_e, T_i, Δn_e, (d) ω_{ITG}, and ω_{ExB}.
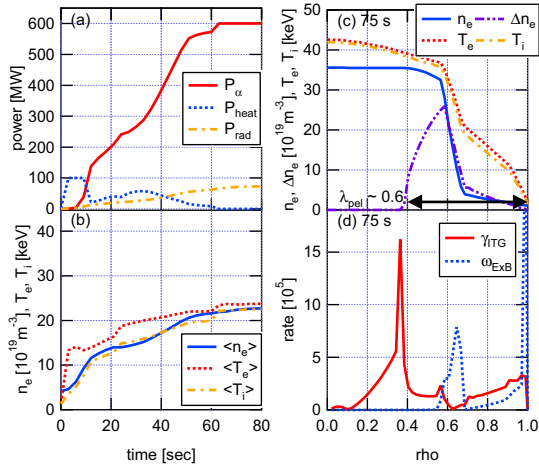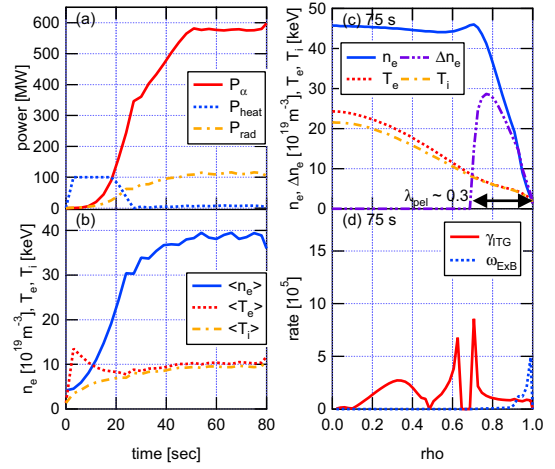

Fig.1 Simulation results of the reversed shear tokamak reactor with the fuelling by the pellet injection. The pellet is penetrated up to $\rho = 0.4$ ("deep penetration case"). It corresponds to the normalized penetration length $\lambda_{pel} = 0.6$. Left figures show the temporal evolutions of (a) the alpha heating power P_α, auxiliary heating power P_{heat}, the radiation power loss P_{rad}, (b) averaged electron density $\langle n_e \rangle$, electron temperature $\langle T_e \rangle$, and ion temperature $\langle T_i \rangle$. Right figures show the radial profiles of (c) electron density n_e, electron temperature T_e, ion temperature T_i, pellet deposition Δn_e, (d) the growth rate of the ion temperature gradient mode ω_{ITG}, and the E x B shearing rate ω_{ExB}.
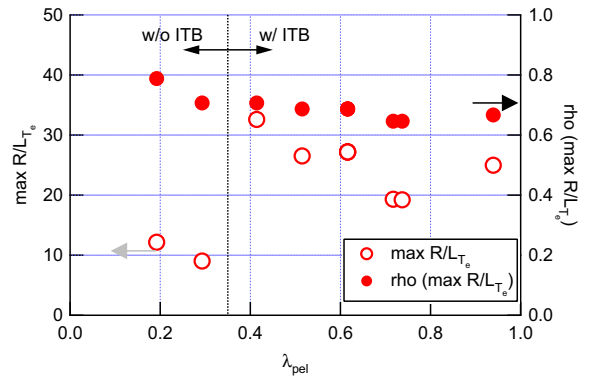

Fig.3 Maximum values of normalized electron temperature gradient R/L_{Te} (open circles) and normalized minor radius ρ where R/L_{Te} peaks (filled circles) for various pellet penetration depths λ_{pel}. ITB is formed in cases where $\lambda_{pel} > 0.35$.

electric field shear at $\rho = 0.65$, ω_{ExB} becomes much larger than γ_{ITG}, and this results in the effective improvement of confinement. This condition can be satisfied by penetrating pellets deeply and by increasing density at the regions inner than $\rho = 0.65$, which determines the threshold pellet penetration depth to form ITB as shown in Fig. 3.
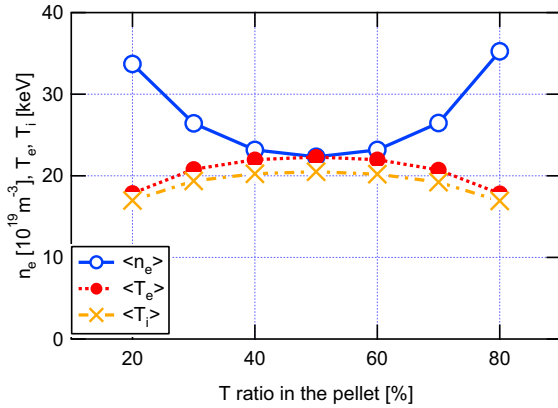

Fig.4 $<n_e>$, $<T_e>$, $<T_i>$ in the steady state in the reversed share tokamak reactor plotted against the tritium ratio in the pellet.
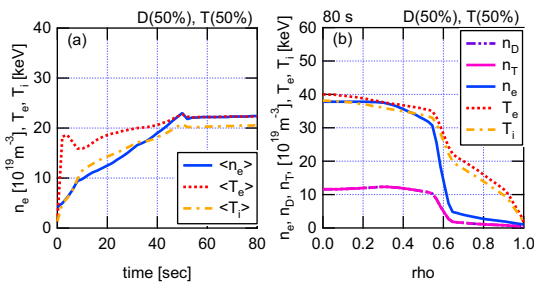

Fig.5   Simulation results of the reversed shear tokamak reactor with fuelling by pellet injection. The pellet composition is 50% deuterium and 50% tritium. (a) Temporal evolutions of $<n_e>$, $<T_e>$, and $<T_i>$. (b) Radial profiles of deuterium ion density n_D, tritium ion density n_T, n_e, T_e, and T_i.
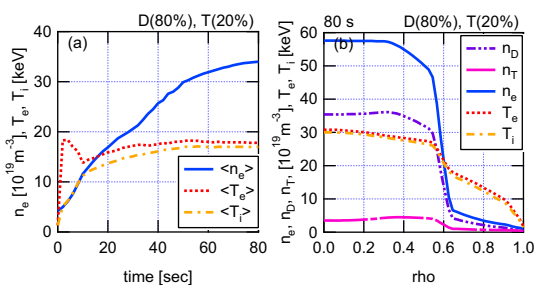

Fig.6   Simulation results of the reversed shear tokamak reactor with fuelling by pellet injection. The pellet composition is 80% deuterium and 20% tritium. (a) Temporal evolutions of $<n_e>$, $<T_e>$, and $<T_i>$. (b) Radial profiles of n_D, n_T, n_e, T_e, and T_i.

3.2. Effect of D/T ratio in the pellet

In the previous section, we decided that a pellet consists of 50% deuterium and 50% tritium. Now we perform a simulation while scanning the density ratio of D/T in the pellet. In this simulation, λ_{pel} is controlled at about 0.7, which satisfies the conditions for forming ITB. Figure 4 shows $<n_e>$, $<T_e>$, and $<T_i>$ in the steady state in the reversed share tokamak reactor plotted against the tritium ratio in the pellet. As the D/T ratio becomes asymmetrical, temperature decreases and higher density is required.

Figure 5 shows the simulation results with the symmetry D/T ratio in the pellet. Both density and temperature have clear ITB. The density profiles between deuterium and tritium are identical. On the other hand, Fig. 6 shows the simulation results with the asymmetry D/T ratio (80% D and 20% T) in the pellet. Although ITB can be observed, the density profiles between deuterium and tritium are quite different. In this case, the short supply of tritium is compensated by increasing the deuterium. Namely, there is a possibility to obtain the required product of deuterium density and tritium density with the operation of a high-density regime, even if the pellet composition is asymmetrical. This suggests it is possible to save the amount of tritium to be used in the reactor by applying appropriate density and temperature.

4. Summary

The efficiency of pellet injection and the relationship between the D/T fuel ratio and plasma parameters were analyzed numerically using the TOTAL (toroidal transport analysis linkage) simulation code. The simulation target was the ITER-like tokamak reactor with the D-T burning plasmas. Deep penetration of the pellet was confirmed to be effective for suppressing anomalous transport and for forming the internal transport barrier. The simulation in which the D/T ratio in a pellet is scanned has revealed that the operational region of temperature and density varies with the D/T ratio. This suggests it is possible to save the amount of tritium to be used in the reactor by using the appropriate operational region.

[1]   K. Yamazaki and T. Amano, Nuclear Fusion **32**, 633 (1992).
[2]   K. Yamazaki *et al.*, Nucl. Fusion **25**, 1543 (1985).
[3]   S. P. Hirshman *et al.*, Comput. Phys. Commun. **43**, 143 (1986).
[4]   Y. B. Kim *et al.*, Phys. Fluids B **3**, 384 (1991).
[5]   A. L. Rogister, Nucl. Fusion **41**, 1101 (2001).
[6]   C. S. Chan and F. L. Hinton, Phys. Fluids **25**, 1493 (1982).
[7]   M. Erba *et al.*, Plasma Phys. Control. Fusion **39**, 261 (1997).
[8]   T. Fujita *et al.*, Phys. Rev. Lett. **78**, 2377 (1997)
[9]   Y. Higashiyama *et al.*, Plasma Fusion Res. **3**, S1048 (2008).

[10] T. S. Harm and K. H. Burrell, Phys. Plasmas **2**, 1648 (1995).

[11] W. A. Houlberg *et al.*, Phys. Plasmas **4**, 3231 (1997).

[12] L. R. Bayler *et al.*, Fusion Technol. **34**, 425 (1998).

[13] P. Parks *et al.*, Nucl. Fusion **17**, 539 (1977).

[14] A. R. Polevoi and M. Shimada, Plasma Phys. Control. Fusion **43**, 1525 (2001).

[15] K. Yamazaki *et al.*, Fusion Engineering and Design **81**, 2743 (2006).